Synthesizing Hypercrosslinked Polymers with Deep Eutectic Solvents to Enhance CO2/N2 Selectivity

ChemSusChem

Chemistry–Sustainability–Energy–Materials

Chemistry Europe

European Chemical Societies Publishing

Accepted Article

Title: Synthesizing Hypercrosslinked Polymers with Deep Eutectic Solvents to Enhance CO2/N2 Selectivity

Authors: Liang Ding, nadhita chanchaona, Kristina Konstas, Matthew Hill, Xianfeng Fan, Colin Wood, and Cher Hon Lau

To be cited as: *ChemSusChem* **2024**, e202301602

Link to VoR: https://doi.org/10.1002/cssc.202301602

WILEY VCH

10.1002/cssc.202301602

WILEY VCH

RESEARCH ARTICLE

Synthesizing Hypercrosslinked Polymers with Deep Eutectic Solvents to Enhance CO_2/N_2 Selectivity

Liang Ding,[a] Nadhita Chanchaona,[a] Kristina Konstas,[b] Matthew R. Hill,[b] Xianfeng Fan,[a] Colin D. Wood,[c] and Cher Hon Lau*[a]

[a] Miss L. Ding, Prof. X. Fan, Dr. C. H. Lau
School of Engineering
The University of Edinburgh
Kings Building, Edinburgh,EH93FB, United Kingdom
E-mail: L.Ding-9@sms.ed.ac.uk , X.Fan@ed.ac.uk , cherhon.lau@ed.ac.uk

[b] Dr. K. Konstas, Prof. M. R. Hill
Manufacturing Unit
CSIRO Australia
Gate 3 Normanby Road, VIC 3141

[c] Prof. Colin D. Wood
Energy Business Unit
CSIRO Australia
Kensington, WA 6151, Australia

Supporting information for this article is given via a link at the end of the document.

Abstract: Hypercrosslinked polymers (HCPs) are widely used in ion exchange, water purification, and gas separation. However, HCP synthesis typically requires hazardous halogenated solvents e.g., dichloroethane, dichloromethane and chloroform which are toxic to human health and environment. Herein we hypothesize that the use of halogenated solvents in HCP synthesis can be overcome with deep eutectic solvents (DES) comprising metal halides – $FeCl_3$, $ZnCl_2$ that can act as both the solvent hydrogen bond donor and catalyst for polymer crosslinking *via* Friedel Crafts alkylation. We validated our hypothesis by synthesizing HCPs in DESs *via* internal and external crosslinking strategies. $[ChCl][ZnCl_2]_2$ and $[ChCl][FeCl_3]_2$ was more suitable for internal and external hypercrosslinking, respectively. The specific surface areas of HCPs synthesized in DES were 20 – 60 % lower than those from halogenated solvents, but their CO_2/N_2 selectivities were up to 453 % higher (CO_2/N_2 selectivity of poly-α,α'-dichloro-p-xylene synthesized in $[ChCl][ZnCl_2]_2$ *via* internal crosslinking reached a value of 105). This was attributed to the narrower pore size distributions of HCPs synthesized in DESs.

Introduction

Hypercrosslinked polymers (HCPs) are nanoporous materials widely used as ion exchange resins for wastewater treatment, metals recovery and water purification, and as sorbents for chromatography.[1] In recent years, HCPs have also been widely studied for gas storage,[2] catalysis and carbon capture. The widespread application and potential of HCPs come from their tailorable pore size as a function of synthesis parameters, monomer choice, thermochemical stability, and low cost.[3] As such, the global market for HCPs is expected to reach $2 billion by 2028 with the emergence of various HCPs reported.[4] This projected growth in HCP demand brings on an unexpected problem – the generation of hazardous solvent waste arising from using halogenated solvents during HCP synthesis.

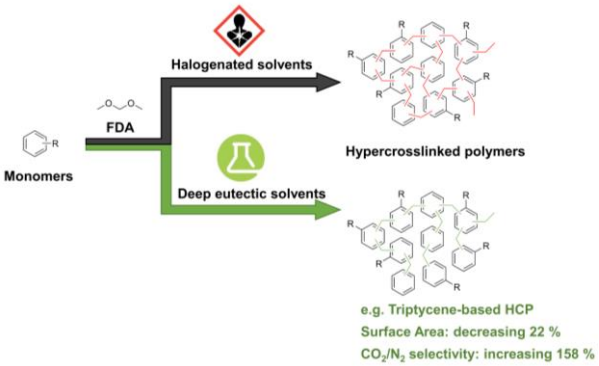

Figure 1. Comparison of traditional protocols that use halogenated solvents and our approach of using deep eutectic solvents to synthesize HCPs.

Underpinned by Friedel-Crafts alkylation, a typical HCP synthesis protocol requires halogenated solvents to initiate and promote the transfer of charged halides from Lewis acid catalysts such as $FeCl_3$, $AlCl_3$, $SnCl_4$ to link up substrates *via* the formation of methylene bridges using internal electrophiles or external crosslinkers e.g., formaldehyde dimethyl acetal (FDA) (Figure 1).[5] Depending on the substrate, HCP synthesis can be achieved by: (1) internal and (2) external crosslinking where electrophiles on the monomer and additional reagents are used for forming methylene bridges that link up monomers, respectively and (3)

post-crosslinking where polymers are crosslinked *via* internal electrophiles.[6]

The mainstream research in the field of HCPs focus on preparing new materials that have remarkable specific surface areas and outstanding performance in separation applications.[3, 7] A new research direction in HCPs is to improve the sustainability of HCP synthesis. Examples of such approaches include solvent-free mechanochemical synthesis,[8] thermal-induced polymerization of a tetrahedral monomer bearing four maleimide pendant groups without using any catalysts and initiators,[9] replacing metal halide Lewis acid catalysts with metal-free Brønsted acids,[10] or replacing the halogenated solvent with benign solvents such as sulfolane.[11] Sulfolane, an organosulfur solvent, which is commonly used in industrial chemical reactions, has demonstrated its feasibility in producing highly porous HCPs from biobased monomers. Considering safety, health, and environmental risks, sulfolane is less toxic than the frequently utilized DCE, as per guidelines for solvent selection.[12] This approach enhanced the sustainability of HCP synthesis and fine-tuned the pore structure for improved CO_2 capture.

A potential alternative is deep eutectic solvents (DES) that comprise a hydrogen bond acceptor (HBA) e.g., a quaternary ammonium salt like chloline chloride (ChCl) and hydrogen bond donor (HBD) e.g., metal halides like $ZnCl_2$, $FeCl_3$[13] to drive Friedel-Crafts reactions[14] between discrete molecules and monomers. For example, Wang and co-workers[15] deployed a range of DESs comprising chloline chloride (ChCl) to catalyze reactions between aldehydes and electron-rich arenes to yield triarylmethanes and diarylalkanes *via* Friedel-Crafts alkylation. This is the same chemistry underpinning polymer hypercrosslinking in HCP synthesis. However, this has not been demonstrated in macromolecular reactions, even though it is feasible.

Here we synthesized HCPs using $[ChCl][ZnCl_2]_2$ and $[ChCl][FeCl_3]_2$ DESs *via* internal and external crosslinking. Although reports have shown that $[ChCl][ZnCl_2]_2$ is toxic for the aquatic environment,[16] its toxicity is still 500-fold less than that of dichloroethane.[17] From this point, $[ChCl][ZnCl_2]_2$ can be regarded as a good substitute for dichloroethane (DCE) during organic synthesis. To the best of our knowledge, this is the first known work that realized the synthesis of HCPs using DESs as both the solvent and catalysts. $ZnCl_2$ and $FeCl_3$ are preferred here as these metal halides are highly efficient for catalyzing polymer hypercrosslinking. The metal halides functioned as both the HBD component of the solvent and as catalysts during Friedel-Crafts alkylation of α,α'-dichloro-p-xylene (DCX), 4,4′-bis(chloromethyl)-1,1′-biphenyl (BCMBP), benzyl alcohol(BA), 1,3,5-triphenylbenzene (TPB) and triptycene. We observed that the use of DES to synthesize HCPs reduced both pore volume and size when compared to HCPs yielded in DCE, as shown in Figure 1. However, the narrower pore size distribution was also key to increasing CO_2/N_2 selectivity from 14 to 105 at 273 K, demonstrating the advantage of synthesizing HCPs in DES. We also exploited the water solubility of the DES components used here, ChCl and metal halides, to facilitate the post-treatment of obtained HCPs products. Apart from the advantages of sustainability and yielding highly selective HCPs, DES also exhibited a minor economic benefit. Based on simple calculations and prices of reagents used in this work, the cost of synthesizing 1 g of *p*-DCX reached £2.37/per batch while conventional DCE method costs £2.49. Outcomes from this work can potentially open up new polymerization applications for DESs and transform HCP synthesis into a more benign process.

Results and Discussion

HCPs synthesis via internal crosslinking with DES

HCP synthesis *via* internal crosslinking is limited to self-polymerizing small molecules comprising bis(chloromethyl), bis(bromomethyl) and hydroxy groups.[18] Cooper and co-workers[19] reported that the Bruanuer-Emmett-Teller (BET) surface areas of HCPs derived from DCX and BCMBP in DCE and using $FeCl_3$ i.e., *p*-DCX and *p*-BCMBP reached 1431 and 1874 $m^2 \cdot g^{-1}$, respectively. As such, we chose these monomers to demonstrate the feasibility of HCP synthesis *via* internal crosslinking using $[ChCl][ZnCl_2]_2$ and $[ChCl][FeCl_3]_2$ DES. We synthesized a series of HCPs as a function of DES component molar ratio i.e., HBA: HBD and reaction time (Table 1).

Table 1. The results of HCPs formed in different DESs via internal hypercrosslinking

Sample	Monomer	DES/Solvents	Temperature (°C)	Molar ratio (monomer: metal halide)	Reaction time	Surface area (m^2/g)
1	DCX	$[ChCl]\ [ZnCl_2]_2$	100	1:28	24h	106
2	DCX	$[ChCl]\ [ZnCl_2]_2$	100	1:28	72h	409
3	DCX	$[ChCl]\ [ZnCl_2]_2$	100	1:50	24h	477
4	DCX	$[ChCl]\ [ZnCl_2]_2$	100	1:8	24h	6
5	DCX	$[ChCl][FeCl_3]_2$	100	1:28	24h	1.6
6	DCX	$[ChCl][FeCl_3]_2$	100	1:8	24h	2.7
7	DCX	$[ChCl][FeCl_3]_2$	100	1:8	72h	3.0
8	DCX	DCE ($ZnCl_2$)	100	1:3	24h	No product
9	DCX	DCE ($FeCl_3$)	100	1:3	24h	964

10	BCMBP	[ChCl] $[ZnCl_2]_2$	100	1:28	24h	35
11	BCMBP	[ChCl] $[ZnCl_2]_2$	100	1:28	72h	143
12	BCMBP	DCE ($ZnCl_2$)	100	1:3	24h	852
13	BCMBP	DCE ($FeCl_3$)	100	1:3	24h	1519

From these reactions, we were able to obtain dark brown particulates that were insoluble in DCE, DCM, and chloroform. This indicated crosslinked DCX and BCMBP. This was validated with solid-state ^{13}C NMR analysis (Figure 2a, S2†). The ^{13}C NMR spectra of *p*-DCX and *p*-BCMBP contained characteristic peaks centered at 128 and 140 ppm, corresponding to non-substituted aromatic carbons and substituted aromatic carbons, respectively. The minor resonance around 50 ppm was correlated to chloromethylene carbons. Compared to the NMR spectrum of unreacted DCX monomers, we observed additional peaks at 36 and 66 ppm in the NMR spectra of *p*-DCX. The peak centered at 36 ppm indicated the presence of methylene bridges that linked up the aromatic rings of the substrates to form polymeric networks, while the peak at 66 ppm correlated to hydroxylmethyl carbons i.e., side products from hydrolysis of chloromethyl groups. Similarly, the peaks for chloromethylene carbons and methylene bridges in the NMR spectra of *p*-BCMBP were located around 45 and 38 ppm. These slight chemical shifts could be caused by the difference in the proportions of di- and trisubstituted benzyl rings.[20] Compared to the NMR spectrum of *p*-DCX in DCE, the peak at 36 ppm of the same polymers yielded in DES studied here were less intense and broader. This peak at 36 ppm has been attributed to unreacted chloromethylene groups.[21] Hence with a less intense and broader peak at 36 ppm, it appeared that the crosslinking degree in HCPs synthesized in DESs were lower than those synthesized in DCE.

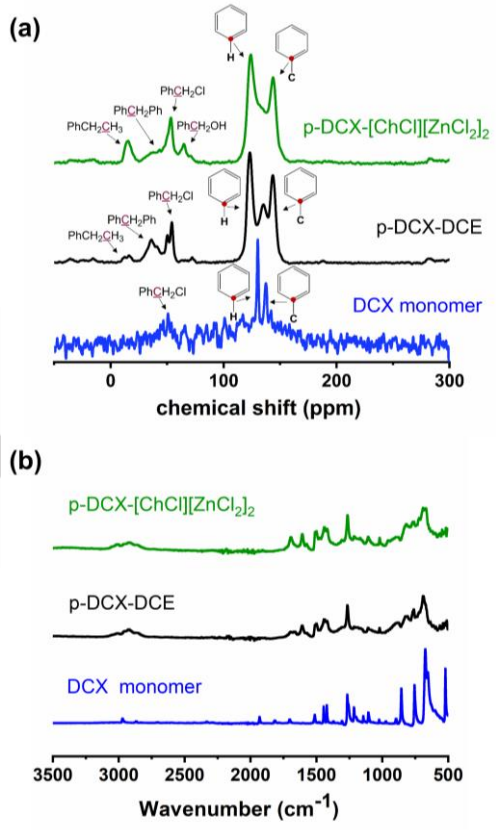

Figure 2. (a) NMR, and (b) FTIR spectra of DCX monomer (blue), p-DCX in [ChCl] $[ZnCl_2]_2$ (green) and DCE (black) for 24h

The FTIR spectra of *p*-DCX and *p*-BCMBP synthesized in DESs were similar to those produced in DCE (Figure 2b, S2†), indicating formation of methylene crosslinking bridges. There were several differences between the FTIR spectra of unreacted monomers and their corresponding polymers. New peaks centered at 2925 and 2853 cm^{-1} in the spectra of *p*-DCX and *p*-BCMBP corresponded to stretching vibrations of methylene groups, bands around 1465 cm^{-1} correlated to C-H bending vibrations of methylene groups and peaks at 1600, 1570 and 1500 cm^{-1} were attributed to the stretching of aromatic C=C bonds. Meanwhile, the strong peak centered at 860 cm^{-1} corresponding to the C-H bending vibrations from bis-substituted aromatic rings diminished upon polymerization. Both NMR and FTIR analyses indicated the formation of multi-substituted aromatic rings linked by methylene bridges.

We measured the nitrogen adsorption isotherms of *p*-DCX and *p*-BCMBP synthesized *via* internal crosslinking in [ChCl]$[ZnCl_2]_2$ and [ChCl]$[FeCl_3]_2$ at 77 K (Table 1). The BET surface areas of *p*-DCX and *p*-BCMBP synthesized in [ChCl]$[FeCl_3]_2$ were negligible. This was despite varying monomer molar percentage, and reaction times, from 6.7 mol.% to 20 mol.%, and 24 h to 72 h, respectively. Meanwhile, the N_2 adsorption isotherms of HCPs synthesized in [ChCl]$[ZnCl_2]_2$ corresponded to a Type I curve that is associated with microporous materials based on IUPAC classification,[22] where we observed a steep rise of N_2 uptake at low relative pressure ($P/P_0 < 0.01$, Figure S3a†), revealing the presence of abundant micropores.[23] We observed that increasing reaction time in [ChCl]$[ZnCl_2]_2$, from 24 h to 72 h, enhanced BET surface areas of *p*-DCX by 4-fold, reaching 409 $m^2\ g^{-1}$. This was still 58 % lower than that of *p*-DCX synthesized in DCE catalyzed by $FeCl_3$. We also synthesized *p*-DCX in DCE using $ZnCl_2$. However, the obtained solid products were easily dissolved in acetone, indicating that these were most likely to be lightly crosslinked oligomers. This could be ascribed to inferior catalytic effects of $ZnCl_2$ in halogenated solvents.[24] This was confirmed here by comparing the BET surface areas of HCPs synthesized in DCE but using $ZnCl_2$ (Samples 8 and 12) and $FeCl_3$ (Samples 9 and 13). Regardless of monomers used, DCX of BCMBP, the BET surface areas of HCPs that were synthesized with $ZnCl_2$ were lower than those synthesized with $FeCl_3$. As BET surface areas are generated as a function of crosslinking degree, a lower crosslinking degree in HCPs is associated with lower BET surface areas.[25] These results suggested that DCX is more reactive in [ChCl]$[ZnCl_2]_2$ than in DCE when the same metal halide is used. One reason why $ZnCl_2$-based DES was effective for HCP synthesis was the molar ratio between metal halide catalysts and substrate (3:1 in traditional protocols that use halogenated solvents, and 28:1 in our approach using DES).

The molar ratio between metal halide: substrate not only impacted the polymerization but also HCP BET surface areas. At molar ratio 8:1, there were insufficient metal halides and excessive substrates in the DES, impeding monomer dissolution and subsequent crosslinking reactions. Increasing the metal halide: substrate molar ratio to 50:1, the BET surface area of the resultant *p*-DCX further increased to 477 m^2 g^{-1}. This meant that more metal halides were available for promoting crosslinking, and this was as effective as prolonging the reaction time. At the same synthetic conditions, the BET surface area of *p*-BCMBP-72h was 66 % lower than that of *p*-DCX-72h, reaching only 143 m^2 g^{-1}. This value was only 17 % of that of *p*-BCMBP synthesized in DCE catalyzed by $ZnCl_2$. This differed from the trends observed in the work of Cooper and co-workers[19] where the BET surface areas of BCMBP-based networks were 24 % higher than DCX-based networks as BCMBP molecules were more likely to construct rigid para geometry between aryl rings that generated more porosity in halogenated solvents. The reactivity of monomers varies in the DCE and DES, which cannot be predicted accurately based on prior knowledge.

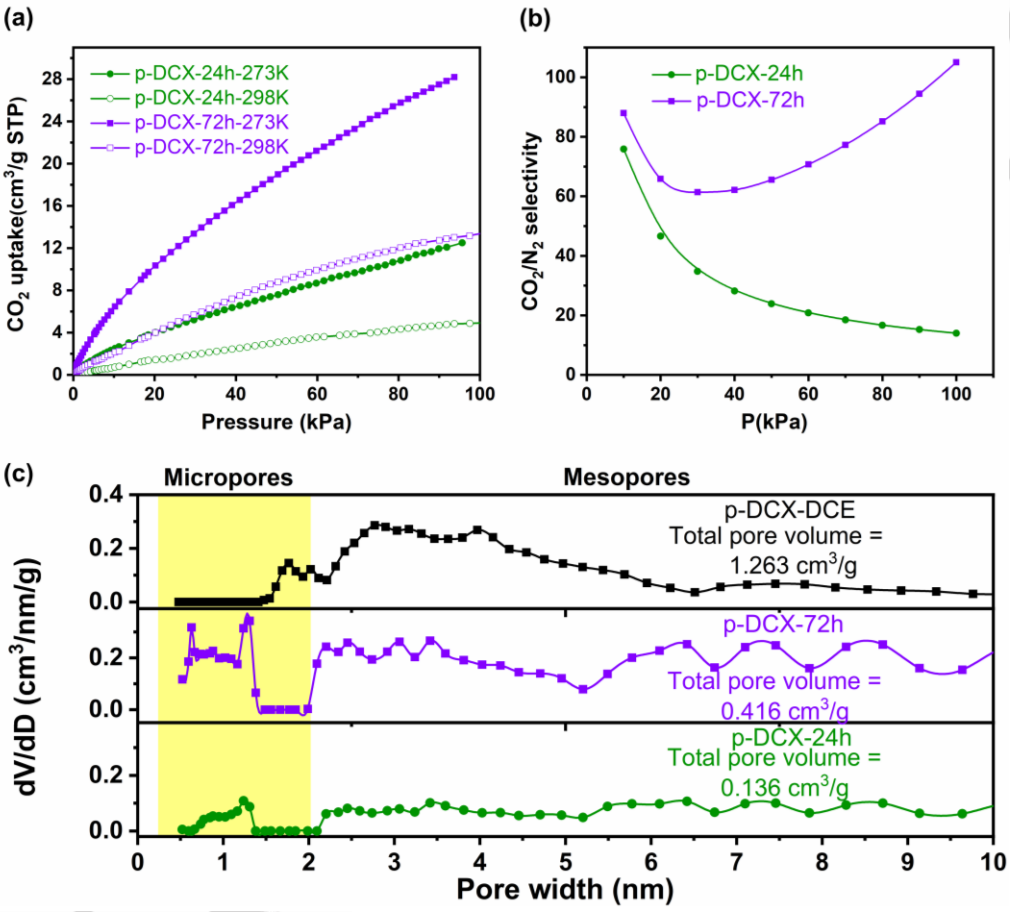

Figure 3. (a)CO_2 uptake of *p*-DCX-24h and *p*-DCX-72h that synthesized in $[ChCl][ZnCl_2]_2$, the isotherms were obtained under 273 K and 298 K, (b) CO_2/N_2 selectivity of *p*-DCX HCPs at 273 K calculated using the IAST theory (CO_2: N_2 = 15: 85), (c) Comparison of the pore size distributions of *p*-DCX HCPs synthesized in DCE and $[ChCl][ZnCl_2]_2$ for 24h and 72h respectively

It was observed that *p*-DCX-72h led to higher CO_2 uptakes and CO_2/N_2 selectivity when compared to *p*-DCX-24h (Figure 3a, 3b). At 273 K, the CO_2 uptake of *p*-DCX-72h reached 28 cm^3 g^{-1}, more than double of that of *p*-DCX-24h. Here we used the ideal adsorption solution theory (IAST) to determine the CO_2/N_2 of these HCPs using a gas mixture comprising 15 % CO_2 and 85 % N_2 (more details in ESI†, Table S1†). At 100 kPa and 273 K, the CO_2/N_2 selectivity of *p*-DCX-72h reached 105, more than 7 times that of *p*-DCX-24h and 5.5-fold higher than that of *p*-DCX synthesized in DCE despite the CO_2 uptake of the latter *p*-DCX type reached 76 cm^3 g^{-1}.[26] Interestingly, the CO_2/N_2 selectivity of *p*-DCX-72h started to increase after P>20 kPa as the effective kinetic diameter of CO_2 (3.3 Å) is smaller than that of N_2 molecules (3.8 Å). This is consistent with the previous findings that the adsorbed amounts of binary gas mixture are dominated by the adsorption strength of the individual species under dilute concentrations while the adsorption selectivity shifts toward the smaller molecules at high pressure.[27] The pore size distributions of *p*-DCX synthesized in $[ChCl][ZnCl_2]_2$ showed that the proportion of micropores (between 0 – 2 nm) in HCPs synthesized over 72 hours was significantly higher than those produced over 24 hours (Figure 3c). These micropores were mainly centered at

0.67, 0.98, and 1.3 nm. This could be attributed to the significant increase in the reaction time, which enabled the formation of ultra-micropores. Compared with *p*-DCX synthesized in DCE using traditional method, *p*-DCX-72h synthesized in $[ChCl][ZnCl_2]_2$ demonstrated a higher abundance of micropores. This is evident from the fact that in *p*-DCX-DCE, the first peak emerged at approximately 1.75 nm. Table S1 compared the textural properties of HCPs synthesized in DES systems and DCE respectively. In the *p*-DCX-DCE, micropores only accounted for 3.38 % while this proportion was improved greatly in *p*-DCX-24h and *p*-DCX-72h, reaching 17.79 % and 27.96 % respectively. Per the previous study, there is a corresponding increase in the BET surface area with the degree of crosslinking intensifying, primarily ascribed to the formation of pore.[28] Despite *p*-DCX HCPs synthesized in DES have inferior surface area, they demonstrated their superiority in the formation of narrower micropores. We also observed the presence of mesopores and macropores, confirming hierarchical porosity in these materials.[29] The substantial difference in micropore distribution between HCPs synthesized using DCE and DES could come from the different reaction kinetics. In conventional batch synthesis of HCPs with DCE solvents, crosslinking reactions are typically completed within two hours, leading to the fast development of irregular linking bridges between intermolecular polymer chains.[30]

In the case of DES reacting system, slower reaction rate is favorable for the establishment of micropores. These data provide valuable insights into the intricate process of porosity development within HCPs. They suggest that porosity in HCPs is a sequential process where micropores are developed first and specific experimental conditions affect the creation of these micropores. Generally, the higher BET surface area and narrower pore size distribution of *p*-DCX-72h contribute to its higher CO_2 uptakes and superior CO_2/N_2 selectivity. The isoteric heat (Qst) of CO_2 adsorption in *p*-DCX synthesized in DES here was reduced with an increase in the amount of CO_2 adsorbed (Figure S3b†), suggesting that adsorption sites were heterogenous.[31] We also observed a 20 kJ mol^{-1} enhancement in isosteric heat of CO_2 adsorption as synthesis time increased from 24 to 72 hours, which was consistent with the observation of increased porosity. Higher Qst value indicated stronger interaction between CO_2 molecules and adsorption sites, benefitting CO_2/N_2 adsorption.[32]

HCPs synthesis via external crosslinking with DES

For external crosslinking in $[ChCl][ZnCl_2]_2$ and $[ChCl][FeCl_3]_2$, we used benzyl alcohol (BA), 1,3,5-triphenylbenzene (TPB) and triptycene as substrates as these monomers yield highly porous HCPs[33] when FDA was deployed as an external crosslinking reagent. The variation of synthesis parameters – reaction duration, molar ratio of substrate: crosslinker: catalyst are listed in Table 2. Generally, $[ChCl][FeCl_3]_2$ was a better medium for external crosslinking of monomers, where HCPs could be synthesized at lower temperatures and over shorter durations. Amongst them, triptycene proved to be the most active where surface areas of *p*-triptycene reached 969 m^2 g^{-1}, the highest amongst all HCPs studied in this work.

Table 2. The results of HCPs formed in different DESs via external hypercrosslinking

Sample	Monomer	Crosslinker	DES/Solvents	Temperature(°C)	Molar ratio (monomer:metal halide:crosslinker)	Reaction time	Surface area (m^2/g)
1	TPB	FDA	$[ChCl][ZnCl_2]_2$	100	1:8:8	24h	No product
2	TPB	FDA	$[ChCl][ZnCl_2]_2$	150	1:8:8	24h	No product
3	TPB	FDA	$[ChCl][ZnCl_2]_2$	180	1:8:8	24h	44
4	TPB	FDA	$[ChCl][FeCl_3]_2$	100	1:8:8	24h	9
5	TPB	FDA	$[ChCl][FeCl_3]_2$	150	1:8:8	24h	172
6	TPB	FDA	$[ChCl][FeCl_3]_2$	100	1:8:8	72h	4
7	TPB	FDA	DCE ($FeCl_3$)	80	1:9:9	24h	1418
8	Triptycene	FDA	$[ChCl][ZnCl_2]_2$	100	1:8:8	24h	No product
9	Triptycene	FDA	$[ChCl][ZnCl_2]_2$	180	1:8:8	24h	426
10	Triptycene	FDA	$[ChCl][FeCl_3]_2$	100	1:8:8	6h	588
11	Triptycene	FDA	$[ChCl][FeCl_3]_2$	100	1:8:8	12h	770
12	Triptycene	FDA	$[ChCl][FeCl_3]_2$	100	1:8:8	24h	969
13	Triptycene	FDA	$[ChCl][FeCl_3]_2$	100	1:8:8	72h	611
14	TPB,Triptycene (1:1)	FDA	$[ChCl][FeCl_3]_2$	100	1:8:8	24h	121
15	Triptycene	FDA	DCE ($FeCl_3$)	80	1:3:3	24h	1469
16	BA	FDA	$[ChCl][ZnCl_2]_2$	150	1:8:8	24h	245
17	BA	FDA	$[ChCl][FeCl_3]_2$	150	1:8:8	24h	384

Solid state ^{13}C NMR analyses showed that the chemical structures of *p*-triptycene synthesized in $[ChCl][FeCl_3]_2$ over 24 and 72 hours were similar (Figure 4a). We observed two intrinsic peaks corresponding to protonated aromatic carbons (125 ppm)

and substituted aromatic carbons (144 ppm) in the NMR spectra of triptycene monomers. In the ^{13}C NMR spectrum of poly-triptycene, we also observed an additional peak centered at 36 ppm that could be attributed to methylene bridge carbons, indicating that crosslinking of triptycene in $[ChCl][FeCl_3]_2$ was feasible. Furthermore, the carbon resonance signals at 49 and 65 ppm were correlated to chloromethyl carbons and hydromethyl groups, indicating that chloromethylation and hydrolysis side reactions might occur during HCP formation, respectively. We also compared the FTIR spectra of triptycene monomer, *p*-triptycene synthesized in $[ChCl][FeCl_3]_2$ and DCE (Figure 4b). The spectra of *p*-triptycene synthesized in $[ChCl][FeCl_3]_2$ and DCE were consistent. The broad peak around 3450 cm^{-1} was attributed to the stretching vibrations of water in the sample. The peak centered at 1460 cm^{-1} could be attributed to C-H bending vibrations of methylene groups, revealing the successful formation of crosslinks comprising methylene bridges.

The N_2 adsorption isotherms of *p*-triptycene synthesized in $[ChCl][FeCl_3]_2$ (Figure S4a†) exhibited a rapid rise under low relative pressure, suggesting the presence of significant micropores in these HCPs. The BET surface areas of *p*-triptycene HCPs increased by 65 %, from 588 m^2 g^{-1} to 969 m^2 g^{-1}, as synthesis duration increased from 6 to 24 hours. As reaction time was further increased to 72 hours, the BET surface area was reduced by 37 %, reaching 611 m^2 g^{-1}. This trend reverse can be attributed to the excessively hypercrosslinking in the HCPs, leading to the partial collapse of micro- and mesopores.[34] It indicated that triptycene is more reactive than DCX as it can be fully crosslinked within 72 hours (about 3 days) while DCX requires more time. Apart from this turning point, the trends in BET surface areas and pore size distributions of *p*-triptycene were similar to those of *p*-DCX and *p*-BCMBP synthesized in $[ChCl][ZnCl_2]_2$ via internal crosslinking. This was also why the CO_2 uptake of *p*-triptycene-24h reached 64 cm^3 g^{-1} at 273 K, the highest amongst all HCPs studied in this work (Figure 5a).

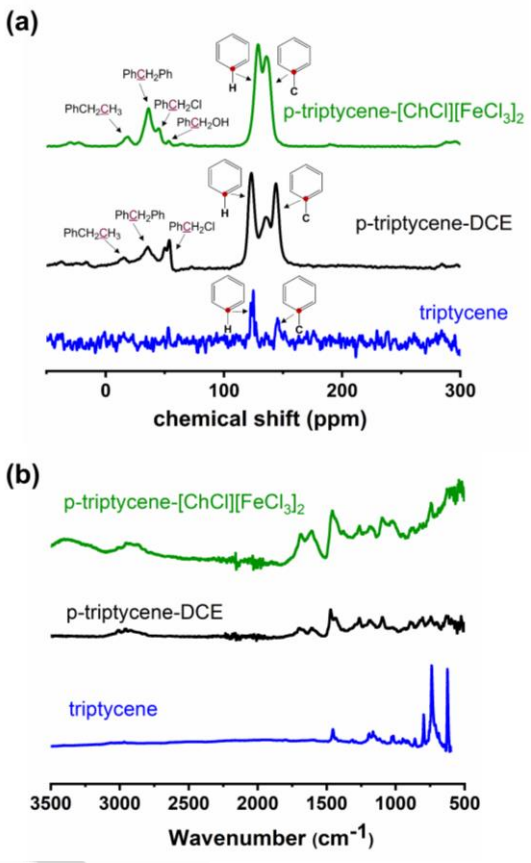

Figure 4. (a) NMR, and (b) FTIR spectra of triptycene monomer (blue), p-triptycene synthesized in [ChCl] $[FeCl_3]_2$ (green) and DCE (black) for 24h

However, the CO_2/N_2 selectivity of *p*-triptycene-24h increased with the increasing pressure. This abnormal trend could be attributed to the inaccurate Langmuir equation that failed to fully fit the N_2 isotherm, bringing errors to consequent IAST selectivity calculations.[27] In addition, its CO_2/N_2 selectivity at 273 K (based on IAST theory and a gas mixture comprising 15 % CO_2 and 85 % N_2) was 13 % lower than those of *p*-triptycene-72h at 100 kPa (Figure 5b). This can be explained by narrower micropore size distribution of *p*-triptycene-72h of which micropores centred at 0.61, 0.85 and 1.85 nm (Figure 5c), contributing to its better CO_2/N_2 selectivity. Comparatively, the micropores of *p*-triptycene-24h mostly distributed around 0.52, 1.02, 1.23 and 1.98 nm. It meant narrower pores in *p*-triptycene were more likely to be retained when excessive hypercrosslinking took place. As for *p*-triptycene-DCE, it had adequate mesopores centred around 3.8 nm in addition to abundant micropores that centred around 0.53, 1.4 and 1.74 nm. By calculating the micro-porosity of the three *p*-triptycene HCPs, *p*-triptycene-72h exhibited the highest value up to 59.23 % despite its reduced total pore volume. These results reflected findings from an earlier work where it was shown that high BET surface areas do not necessarily correlate to high CO_2/N_2 selectivities.[35] Instead, a trade-off effect between CO_2 uptake and CO_2/N_2 selectivity existed in most porous materials i.e., increased CO_2 selectivity is usually accompanied with lower CO_2 uptake, consistent with the behavior of *p*-triptycene-72h.[36] The CO_2/N_2 selectivities of *p*-triptycene-24h and *p*-triptycene-72h

reached 99 and 75, respectively, higher than those produced in halogenated solvents (52).[37] Overall, the findings of external hypercrosslinking are consistent with the results we summarized from internal hypercrosslinking. It means DES reaction systems excel in yielding narrower pore structures and thus enhancing gas selectivity. Moreover, excessive cross-linking is not inherently undesirable because it can be fine-tuned to create narrower pores as required. The isosteric heat of CO_2 adsorption (Qst) of *p*-triptycene-24h and *p*-triptycene-72h (Figure S4b†) were similar, with Qst of the latter material 2.3 % higher, conforming to its better CO_2/N_2 selectivity.

We were also able to crosslink TPB using the same synthetic conditions at 100 °C (Table 2) but the BET surface areas of *p*-TPB synthesized in DESs were negligible. This was despite record BET surface areas of *p*-TPB based HCPs synthesized in halogenated solvents (1700 to 2400 $m^2\ g^{-1}$).[38] A comparison between the FTIR spectrum of *p*-TPB prepared in $[ChCl][FeCl_3]_2$ with that of TPB monomer (Figure S5†) showed that these spectra were identical with a few new, but subtle peaks appearing after Friedel-Crafts alkylation. Peaks above 3000 cm^{-1} could be assigned to stretching vibrations of aromatic C-H bonds, while peaks around 1593, 1485 cm^{-1} were correlated to aromatic C=C stretching. Both spectra also contained characteristic adsorption bands at 876, 747 and 683 cm^{-1} that corresponded to C-H bending vibrations, indicating the presence of 1,3,5-trisubstituted benzene rings. Unlike the FTIR spectra of *p*-TPB synthesized in DCE, the absence of a peak at 1465 cm^{-1} that was correlated to C-H bending vibrations of methylene groups indicated minimal crosslinking of TPB in DESs. When we increased the reaction temperature to 150 °C, we obtained microporous *p*-TPB with BET surface areas reaching 172 $m^2\ g^{-1}$. This meant that TPB monomer could be crosslinked into HCPs in DESs, but at higher temperatures i.e., TPB was less reactive than triptycene. A possible explanation for this contrasting effect of crosslinking triptycene and TPB in DESs could be due to their chemical structures. Triptycene has a paddle wheel structure while TPB is a planar molecule.[37, 39]

To verify this hypothesis, we attempted to synthesize HCPs using equimolar amounts of TPB and triptycene as co-monomers (sample 14 in Table 2). By replacing 50 mol. % of triptycene with TPB, the BET surface area of these copolymerized HCPs only reached 121 $m^2\ g^{-1}$, an 88 % reduction when compared to that of *p*-triptycene (969 $m^2\ g^{-1}$). This suggested that TPB hindered the formation of porous HCPs, and a reactive substrate was required for HCP synthesis in DESs. We also successfully synthesized *p*-BA, but at a higher temperature of 150 °C, in both $[ChCl][ZnCl_2]_2$ and $[ChCl][FeCl_3]_2$ where BET surface areas reached 245 and 384 $m^2\ g^{-1}$, respectively. These results elucidated that DESs evaluated in this work were applicable for crosslinking different monomers while the specific reaction conditions depended on monomer reactivity. Adjusting reaction temperature and reaction time could be exploited to tailor the (micro)porosity of HCPs. In addition, the recovery of iron components in the spent DES was described in ESI†.

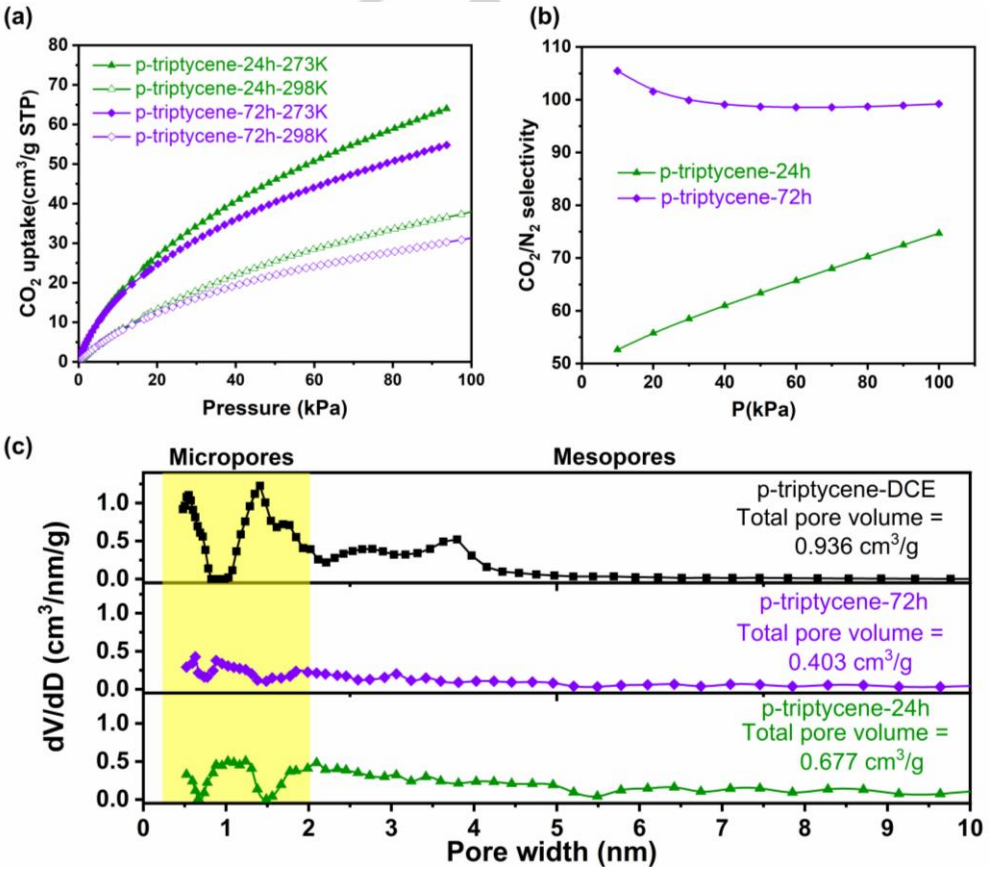

Figure 5. (a) CO_2 uptake of *p*-triptycene-24h and *p*-triptycene-72h that synthesized in $[ChCl][FeCl_3]_2$, the isotherms were obtained under 273 K and 298 K, (b) CO_2/N_2 selectivity of *p*-triptycene HCPs at 273 K calculated using the IAST theory (CO_2: N_2 = 15: 85), (c) Comparison of the pore size distributions of *p*-triptycene HCPs synthesized in DCE and $[ChCl][FeCl_3]_2$ for 24h and 72h respectively

Impacts of textual properties on CO_2 uptake and selectivity

HCPs synthesized in DES systems highlighted their supremacy in the formation of narrower micropores, benefitting the adsorption of CO_2 molecules. Here, we selected six typical HCPs and compared their performance in CO_2 uptake and CO_2/N_2 selectivity (Table 3). Pore structures of HCPs are closely related to the crosslinking degree, which, in turn determine their adsorption behaviors towards different adsorbates. Basically, the CO_2 uptake is directly proportional to the specific surface area. It means high BET surface areas of HCPs ensure their adsorption capacity towards CO_2. When the BET surface area is high, HCPs offer a greater number of active sites and, therefore, a more extensive area for CO_2 molecules to adhere, resulting in increased adsorption capacity. This is supported from the results that HCPs synthesized in DCE generally have higher specific surface areas and corresponding CO_2 uptake.

However, the situation is more complicated when it comes to the CO_2/N_2 selectivity of these HCPs. The textual properties such as specific surface area, pore volumes and pore size distribution, influence the ultimate gas selectivity collectively. All of the six HCPs displayed hierarchical pore distributions comprising both micro and mesopores. Notably, *p*-DCX and *p*-triptycene synthesized in DCE own more proportional mesopores, which could be attributed to the fast reaction kinetics undergoing in the halogenated solvent. These mesopores provide extra convenience for N_2 molecules to penetrate. At the operating adsorption temperature (273 K), CO_2 is recognized to have better accessibility into the narrow micropores because minimum kinetic dimensions of CO_2 (0.33 nm) is smaller than that of N_2(0.36 nm).[40] Therefore, the narrow micropores existing in the *p*-DCX and *p*-triptycene synthesized in DES favor the adsorption of CO_2 but limit the adsorption of N_2 molecules. This explained why *p*-DCX-DCE and *p*-triptycene-DCE possessed comparatively low CO_2/N_2 selectivity despite high BET surface areas. Compared with *p*-DCX-24h and *p*-DCX-72h synthesized in $[ChCl][ZnCl_2]_2$, the latter HCP exhibited both enhanced BET SA and microporosity, consequently resulting in increased selectivity, up to 105. Moving on to the case of triptycene-based HCPs, the pore size distribution of *p*-triptycene-DCE displayed an obvious peak approximately at 3.8 nm in addition to its 50.8 % micropores proportion. This led to its lower CO_2/N_2 selectivity (29) as N_2 molecules could also diffuse into pores without limitations as well. Conversely, *p*-triptycene-24h-$[ChCl][FeCl_3]_2$ do not possess prominent mesopores, and thus it showed an increment of 158 % in CO_2/N_2 selectivity while CO_2 uptake only dropped by 22 %. Excessive crosslinking significantly diminished both BET surface area and pore volume in *p*-triptycene-72h-$[ChCl][FeCl_3]_2$. However, an increasing trend in the CO_2/N_2 selectivity was accompanied with a slight increase in microporosity. This was due to the disappearance of partial mesopores resulting from pore collapse during hypercrosslinking. Their pore size distributions above 2 nm were consistent with this explanation. In this work, narrower micropores were confirmed in the HCPs synthesized in the DESs *via* internal and external hypercrosslinking. The relationship between the textural properties of HCPs and CO_2 adsorption performance was also revealed. The CO_2/N_2 selectivity of HCPs could be improved through adopting new reaction medium such as DESs, adjusting crosslinking degree, *etc.*

Table 3. Comparison of CO_2 uptake, CO_2/N_2 selectivity at 273K and textural properties of six HCPs

Sample	BET SA ($m^2\ g^{-1}$)	CO_2 uptake [a] ($cm^3\ g^{-1}$)	CO_2/N_2 [b] selectivity	Ref
p-DCX-DCE	1063	76	19	[29]
p-DCX-24h-$[ChCl][ZnCl_2]_2$	106	12	14	This work
p-DCX-72h-$[ChCl][ZnCl_2]_2$	409	28	105	This work
p-triptycene-DCE	1246	78	29	[40]
p-triptycene-24h-$[ChCl][FeCl_3]_2$	969	64	75	This work
p-triptycene-72h-$[ChCl][FeCl_3]_2$	611	55	99	This work

[a] CO_2 uptake was obtained under 273K and 1bar. [b] CO_2/N_2 selectivity was calculated using the IAST theory (CO_2: N_2 = 15: 85) at 273K and 1 bar.

DES suitability for various crosslinking strategies

DES choice was crucial for determining the crosslinking strategy. $[ChCl][ZnCl_2]_2$ was more effective for internal crosslinking but not for external crosslinking, where $[ChCl][FeCl_3]_2$ was a better option. This was intriguing as it is widely accepted that $FeCl_3$ is a Lewis acid that is more effective for catalyzing Friedel-Crafts reactions than $ZnCl_2$.[24] However, this was not the case in this work, when $FeCl_3$ functioned as both the catalyst and hydrogen bond donor in $[ChCl][FeCl_3]_2$. This could be ascribed to the difference between the Lewis acidity of these catalysts in ionic liquids. Using pyridine and ethanenitrile as infrared probe molecules, Yang and coworkers[41] observed that interactions between the metal halides in ionic liquids and these probe molecules created shifts in IR absorption bands in the 1400 – 1700 cm^{-1} region for pyridine and 2200-2400 cm^{-1} region for ethanenitrile where subtle shifts in IR absorption bands were observed. For example, a band at 1450 cm^{-1} corresponded to coordination between pyridine and Lewis acid sites, and shifts in this band increased in the order of CuCl <

$FeCl_3$ < $ZnCl_2$ < $AlCl_3$. This indicated that the Lewis acidity of $ZnCl_2$ was stronger than $FeCl_3$ in these ionic liquids. This order was also observed with ethanenitrile and in other ionic liquids comprising imidazole cations and chlorometallate anions.[42]

Here, we hypothesized that these trends could also be observed with the DESs used in this work. This was validated by using Fourier infrared spectroscopy (FTIR) to investigate the Lewis acidity of $[ChCl][ZnCl_2]_2$ and $[ChCl][FeCl_3]_2$. All samples for FTIR characterization were prepared by mixing DES and probe liquid (pyridine) in a given molar ratio of 1:1.[43] The spectra of neat pyridine and mixtures of pyridine and DES are shown in Figure 6. The characteristic single peak of pristine pyridine was centered at 1437 cm^{-1}. In the presence of $[ChCl][ZnCl_2]_2$, the position of this peak shifted to 1450 cm^{-1} while in the case of $[ChCl][FeCl_3]_2$, there was only a small peak around 1449 cm^{-1}. This indicated that the Lewis acidity of $[ChCl][ZnCl_2]_2$ was higher than $[ChCl][FeCl_3]_2$. Considering that this band position shift was minor, all IR spectra were scanned in triplicates with a resolution of 1 cm^{-1} to ensure reliability. The band near 1540 cm^{-1} corresponded to pyridinium ions coordinated to Brønsted acidic sites and was only observed in the spectrum of $[ChCl][FeCl_3]_2$, indicating that $[ChCl][FeCl_3]_2$ was more likely to behave like a Brønsted acid.

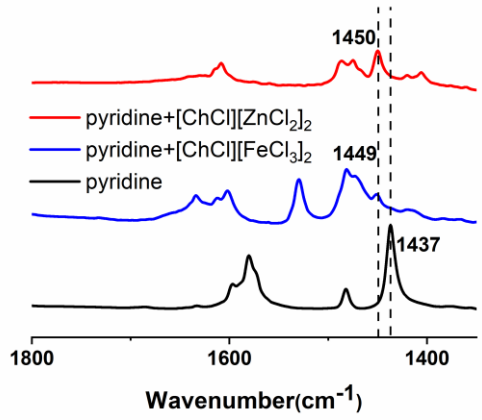

Figure 6. FTIR spectra of (a) pyridine (black), (b)pyridine+$[ChCl][ZnCl_2]_2$ (red), (c) pyridine+ $[ChCl][FeCl_3]_2$ (blue) showing a red-shift in peak position associated with pyridine due to different Lewis acidity

In the case of $[ChCl][ZnCl_2]_2$, $[Zn_2Cl_5]^-$ ions that were mostly detected.[44] These ions could form carbocations comprising aromatic chloromethyl groups and zinc chloride clusters that could then be attacked by the benzene ring of another DCX molecule, forming an intermediate cyclohexadienyl cation. These intermediates could lead to the re-formation of carbon-carbon double bonds that restored aromaticity to the target compound and constructed interchain methylene linkages, forming HCPs *via* internal crosslinking. $[ChCl][ZnCl_2]_2$ was ineffective for external crosslinking where FDA was present and used in chloromethylation prior conversion into methylene bridges that knitted aromatic rings to form highly-crosslinked polymeric networks. $[Zn_2Cl_5]^-$ ions were unable to chloromethylate formaldehyde as well as $[FeCl_4]^-$ species that were mostly detected in $[ChCl][FeCl_3]_2$. This was consistent with the findings of Cao *et al.*[45] in which they proved that between $[ChCl][ZnCl_2]_2$, and $[ChCl][FeCl_3]_2$, only the latter DES type was effective for catalyzing the condensation of 1,4-dialkoxybenzene and paraformaldehyde. Interestingly, for external crosslinking, we observed that HCPs with higher BET surface areas could still be obtained in $[ChCl][ZnCl_2]_2$, but only when higher temperatures and longer durations i.e., harsher experimental conditions were used (Table 2).

Conclusion

Two deep eutectic solvents, $[ChCl][ZnCl_2]_2$ and $[ChCl][FeCl_3]_2$, were proven in this work as feasible alternatives for halogenated solvents commonly used in Friedel-Crafts reactions for the synthesis of HCPs. This work successfully expanded the application of DES in polymerization chemistry and proposed a versatile synthetic strategy for porous HCPs. We demonstrated the feasibility and versatility of this approach using typical monomers that were proven in the past to yield HCPs. We also proposed possible mechanisms for hypercrosslinking process in DESs. $[ChCl][ZnCl_2]_2$ and $[ChCl][FeCl_3]_2$ were suitable for internal and external crosslinking, respectively. Notably, although the specific surface areas of *p*-triptycene HCPs synthesized in DESs were 22 – 52 % lower than those produced in halogenated solvents, their CO_2 uptake only dropped 18 % – 30 %. This can be attributed to the narrower pore size distributions of the former materials, increasing CO_2/N_2 selectivity by up to 450 %. This result further proves that micropores boost the CO_2 adsorption.[46] We believe that the findings from this work would benefit the explorations towards HCPs with ultra-micropores and their applications in gas separation.

Experimental Section

Materials and instruments

Choline chloride, zinc chloride, ferric chloride, 1,2-dichloroethane (DCE), were purchased from Alfa aesar. α,α'-dichloro-p-xylene (DCX), 4,4′-bis(chloromethyl)-1,1′-biphenyl (BCMBP), benzyl alcohol (BA), 1,3,5-triphenylbenzene (TPB), triptycene and formaldehyde dimethyl acetal (FDA) were purchased from Sigma Aldrich. Their chemical structures are shown in Figure S1†. Methanol, acetone, and ethanol were provided by Fisher Scientific. All chemicals were used as received without further purification.

All samples were examined by attenuated total reflectance-Fourier transform infrared spectroscopy (ATR-FTIR) to investigated chemical bonds of HCPs and Lewis acidity of different DES systems. Solid-state Nuclear Magnetic resonance (NMR) was also used to detect the chemical structures of HCPs with a Perkin ava 300M machine. The adsorption and desorption

isotherms of N_2 and CO_2 were obtained from a Micrometrics ASAP 2420 instrument at 77K, 273K and 298K respectively after degassing. Surface morphology of HCPs was determined by scanning electron microscopy (SEM) using a JEOS JSM-IT100 instrument (Figure S8-S10†). The X-ray photoelectron spectroscopy (XPS) measurements were performed with Al mono radiation X-ray source.

Synthesis procedure

Synthesis of deep eutectic solvents (DES)

Two DES were prepared as follows: Choline chloride and zinc chloride (or iron chloride) were mixed directly and stirred at 120 °C for 5h until homogenous solutions formed. The molar ratio of choline chloride and metal chloride is 1:2. The obtained DES were used in the subsequent hypercrosslinking.

Internal hypercrosslinking—Synthesis of *p*-DCX

α,α'-dichloro-p-xylene (DCX, 1 g, 5.71 mmol) were added in the $[ChCl][ZnCl_2]_2$ (32.97 g, 79.97 mmol). The whole reaction was kept at 100 °C for 24 hours. The resulting mixture was washed by water, acetone, and ethanol for three times each. The product was dried in vacuum oven at 100 °C for 12 h and named as poly-DCX. The similar practice was applied when $[ChCl][FeCl_3]_2$ served as solvent. DCX was also hypercrosslinked in DCE as a control group. $FeCl_3$ (2.78 g, 17.1 mmol) was added in the solution of DCX (1g, 5.71 mmol) in anhydrous DCE (30 mL), and the reaction was stirred at 80°C for 24h. The molar ratio of DCX and $FeCl_3$ was 1:3 considering too much catalyst may be detrimental to the SA of final products.[19]

Internal hypercrosslinking—Synthesis of *p*-BCMBP

4,4′-bis(chloromethyl)-1,1′-biphenyl (BCMBP, 1 g, 4 mmol) were added in the $[ChCl][ZnCl_2]_2$ (23.08 g, 56 mmol). The whole reaction was kept at 100 °C for 24 hours. The resulting mixture was washed by water, acetone, and ethanol for three times each. The product was dried in vacuum oven at 100 °C for 12 h and named as poly-BCMBP. The similar practice was applied when $[ChCl][FeCl_3]_2$ served as solvent.

External hypercrosslinking—Synthesis of *p*-TPB

1,3,5-triphenylbenzene (TPB, 1.53 g, 5 mmol) and formaldehyde dimethyl acetal (FDA, 3.04 g, 40 mmol) were added in the $[ChCl][FeCl_3]_2$ (9.28 g, 20mmol). The whole reaction was kept at 100 °C for 24 hours. The resulting mixture was washed by water, DCE and methanol for three times each. The product was dried in vacuum oven at 100 °C for 12 h and named as poly-TPB. The similar practice was applied when $[ChCl][ZnCl_2]_2$ served as solvent.

External hypercrosslinking—Synthesis of *p*-triptycene

Triptycene (1.27 g, 5 mmol) and formaldehyde dimethyl acetal (FDA, 3.04 g, 40 mmol) were added in the $[ChCl][FeCl_3]_2$ (9.28 g, 20 mmol). The whole reaction was kept at 100 °C for 24 hours. The resulting mixture was washed by water, DCE and methanol for three times each. The product was dried in vacuum oven at 100 °C for 12h and named as poly-triptycene. The similar practice was applied when $[ChCl][ZnCl_2]_2$ served as solvent. Triptycene was also hypercrosslinked in DCE as a control group. $FeCl_3$ (2.44 g, 15 mmol) was added in the solution of triptycene (1.27g, 5 mmol) and FDA (1.14 g, 15 mmol) in anhydrous DCE (26 mL), and the reaction was stirred at 80°C for 24h. The molar ratio of triptycene and $FeCl_3$ was 1:3 considering too much catalyst may be detrimental to the SA of final products.[19]

External hypercrosslinking—Synthesis of *p*-BA

Benzyl alcohol (0.541, 5 mmol) and formaldehyde dimethyl acetal (FDA, 3.04 g, 40 mmol) were added in the $[ChCl][FeCl_3]_2$ (9.28 g, 20 mmol). The whole reaction was kept at 100 °C for 24 hours. The resulting mixture was washed by water, DCE and methanol for three times each. The product was dried in vacuum oven at 100 °C for 12h and named as poly-BA. The similar practice was applied when $[ChCl][ZnCl_2]_2$ served as solvent.

Supporting Information

The authors have cited additional references within the Supporting Information.[47]

Keywords: Hypercrosslinked Polymers • Deep Eutectic Solvents • CO_2/N_2 selectivity

Reference

[1] N. Fontanals, M. Galià, P. A. Cormack, R. M. Marcé, D. C. Sherrington, F. Borrull, *J. Chromatogr. A* **2005**, *1075*, 51-56.
[2] Z. Tang, S. Li, W. Yang, X. Yu, *J. Mater. Chem.* **2012**, *22*, 12752-12758.
[3] J. Huang, S. R. Turner, *Polym. Rev.* **2018**, *58*, 1-41.
[4] N. Chanchaona, L. Ding, S. Lin, S. Sarwar, S. Dimartino, A. J. Fletcher, D. M. Dawson, K. Konstas, M. R. Hill, C. H. Lau, *J. Mater. Chem. A* **2023**.
[5] B. Li, R. Gong, W. Wang, X. Huang, W. Zhang, H. Li, C. Hu, B. Tan, *Macromolecules* **2011**, *44*, 2410-2414.
[6] L. Tan, B. Tan, *Chem. Soc. Rev.* **2017**, *46*, 3322-3356.
[7] L. Tan, B. Li, X. Yang, W. Wang, B. Tan, *Polymer* **2015**, *70*, 336-342.
[8] A. M. Borrero-López, A. Celzard, V. Fierro, *ACS Sustain. Chem. Eng.* **2022**, *10*, 16090-16112.
[9] Y. Su, Z. Wang, A. Legrand, T. Aoyama, N. Ma, W. Wang, K.-i. Otake, K. Urayama, S. Horike, S. Kitagawa, *J. Am. Chem. Soc.* **2022**.
[10] L. Prince, P. Guggenberger, E. Santini, F. Kleitz, R. T. Woodward, *Macromolecules* **2021**, *54*, 9217-9222.
[11] F. Björnerbäck, N. Hedin, *ChemSusChem* **2019**, *12*, 839-847.
[12] D. Prat, J. Hayler, A. Wells, *Green Chem.* **2014**, *16*, 4546-4551.
[13] E. L. Smith, A. P. Abbott, K. S. Ryder, *Chem. Rev.* **2014**, *114*, 11060-11082.
[14] N. Azizi, Z. Manocheri, *Res. Chem. Intermed.* **2012**, *38*, 1495-1500.
[15] A. Wang, P. Xing, X. Zheng, H. Cao, G. Yang, X. Zheng, *RSC Adv.* **2015**, *5*, 59022-59026.
[16] I. Juneidi, M. Hayyan, O. Mohd Ali, *Environ. Sci. Pollut. Res.* **2016**, *23*, 7648-7659.

[17] W. W. Johnson, M. T. Finley, *Handbook of acute toxicity of chemicals to fish and aquatic invertebrates: Summaries of toxicity tests conducted at Columbia National Fisheries Research Laboratory, 1965-78, Vol. 137*, US Department of the Interior, Fish and Wildlife service, **1980**.
[18] Y. Luo, S. Zhang, Y. Ma, W. Wang, B. Tan, *Polym. Chem.* **2013**, *4*, 1126-1131.
[19] C. D. Wood, B. Tan, A. Trewin, H. Niu, D. Bradshaw, M. J. Rosseinsky, Y. Z. Khimyak, N. L. Campbell, R. Kirk, E. Stöckel, *Chem. Mater.* **2007**, *19*, 2034-2048.
[20] R. V. Law, D. C. Sherrington, C. E. Snape, I. Ando, H. Kurosu, *Macromolecules* **1996**, *29*, 6284-6293.
[21] H. Park, M. Kang, D. W. Kang, C. S. Hong, *J. Mater. Chem. A* **2022**, *10*, 3579-3584.
[22] Z. A. ALOthman, *Materials* **2012**, *5*, 2874-2902.
[23] K. S. Sing, *Pure Appl. Chem.* **1985**, *57*, 603-619.
[24] C. Xu, L. Jiang, X. Qin, C. Jin, L. Liu, S. Yu, M. Xian, *J. Taiwan Inst. Chem. Eng.* **2019**, *102*, 340-348.
[25] H. Gao, L. Ding, H. Bai, A. Liu, S. Li, L. Li, *J. Mater. Chem. A* **2016**, *4*, 16490-16498.
[26] Y. Sang, J. Huang, *Chem. Eng. J.* **2020**, *385*, 123973.
[27] E. D. Akten, R. Siriwardane, D. S. Sholl, *Energy & Fuels* **2003**, *17*, 977-983.
[28] a) Z. Fu, J. Jia, J. Li, C. Liu, *Chem. Eng. J.* **2017**, *323*, 557-564; b) Q.-Q. Liu, L. Wang, A.-G. Xiao, H.-J. Yu, Q.-H. Tan, *Eur. Polym. J.* **2008**, *44*, 2516-2522.
[29] D. Chen, S. Gu, Y. Fu, Y. Zhu, C. Liu, G. Li, G. Yu, C. Pan, *Polym. Chem.* **2016**, *7*, 3416-3422.
[30] Y. Yang, B. Tan, C. D. Wood, *J. Mater. Chem. A* **2016**, *4*, 15072-15080.
[31] a) T. Watabe, K. Yogo, *Sep. Purif. Technol.* **2013**, *120*, 20-23; b) A. Nuhnen, C. Janiak, *Dalton Trans.* **2020**, *49*, 10295-10307.
[32] a) B. Zhu, S. He, Y. Yang, S. Li, C. H. Lau, S. Liu, L. Shao, *Nat. Commun.* **2023**, *14*, 1697;
b) B. Zhu, Y. Yang, L. Guo, K. Wang, Y. Lu, X. He, S. Zhang, L.Shao, *Angew. Chem. Int. Ed.* **2023**, e202315607.
[33] A. H. Alahmed, M. E. Briggs, A. I. Cooper, D. J. Adams, *J. Mater. Chem. A* **2019**, *7*, 549-557.
[34] a) X. Dong, A. Akram, B. Comesaña-Gándara, X. Dong, Q. Ge, K. Wang, S.-P. Sun, B. Jin, C. H. Lau, *ACS Appl. Polym. Mater.* **2020**, *2*, 2586-2593; b) J. S. M. Lee, M. E. Briggs, T. Hasell, A. I. Cooper, *Adv. Mater.* **2016**, *28*, 9804-9810.
[35] R. Dawson, E. Stöckel, J. R. Holst, D. J. Adams, A. I. Cooper, *Energy Environ. Sci.* **2011**, *4*, 4239-4245.
[36] B. Zhu, S. He, Y. Wu, S. Li, L. Shao, *Engineering* **2023**, *26*, 220-228.
[37] D. Chen, S. Gu, Y. Fu, X. Fu, Y. Zhang, G. Yu, C. Pan, *New J. Chem.* **2017**, *41*, 6834-6839.
[38] X. Xia, P. Sun, X. Sun, Y. Wang, S. Yang, Y. Jia, B. Peng, C. Nie, *e-Polymers* **2022**, *22*, 19-29.
[39] L. Liu, Y. Zang, H. Jia, T. Aoki, T. Kaneko, S. Hadano, M. Teraguchi, M. Miyata, G. Zhang, T. Namikoshi, *Polym. Rev.* **2017**, *57*, 89-118.
[40] R. V. Rios, J. Silvestre-Albero, A. Sepulveda-Escribano, M. Molina-Sabio, F. Rodriguez-Reinoso, *J. Phys. Chem. C* **2007**, *111*, 3803-3805.
[41] Y.-l. Yang, Y. Kou, *Chem. Commun.* **2004**, 226-227.
[42] O. Acevedo, *J. Mol. Graph. Model.* **2009**, *28*, 95-101.
[43] L. Tao, D. Yuefeng, G. Shucai, C. Ji, *Chin. J. Chem. Eng.* **2010**, *18*, 322-327.
[44] a) A. P. Abbott, G. Capper, D. L. Davies, R. Rasheed, *Inorg. Chem.* **2004**, *43*, 3447-3452; b) Q. Fanglong, S. Jinhe, X. Shaolei, S. Chenglong, J. Yongzhong, *Int. Proc. Chem., Biol. Environ. Eng.* **2015**, *90*, 70-75.
[45] J. Cao, Y. Shang, B. Qi, X. Sun, L. Zhang, H. Liu, H. Zhang, X. Zhou, *RSC Adv.* **2015**, *5*, 9993-9996.
[46] S. Wang, Y. Li, S. Dai, D. e. Jiang, *Angew. Chem. Int. Ed.* **2020**, *59*, 19645-19648.
[47] a) M. Karimi, M. B. Lejbini, V. Jahangir, A. S. Jam, S. M. Asl, *Optik* **2019**, *181*, 816-822; b) H. Cui, Y. Liu, W. Ren, *Adv. Powder Technol.* **2013**, *24*, 93-97.

10.1002/cssc.202301602

WILEY VCH

RESEARCH ARTICLE

Entry for the Table of Contents

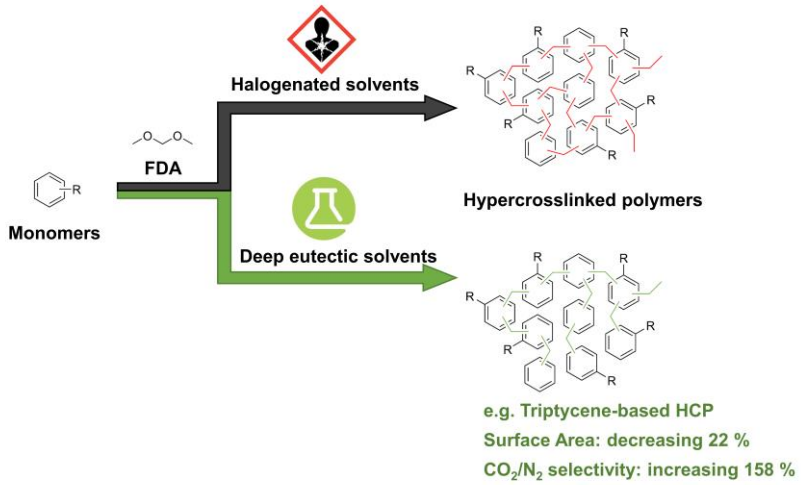

Deep eutectic solvents have been first verified feasible for the synthesis of hypercrosslinked polymers (HCPs) based on Friedel-Crafts chemistry. Different starting monomers are selected and exhibited significantly improved CO_2/N_2 selectivity due to narrower pore size distribution in these HCPs, comparing with HCPs synthesized in conventional halogenated solvents. Especially, triptycene-based HCP demonstrated an increase of 158% in the CO_2/N_2 selectivity with losing only 22% of the surface area.